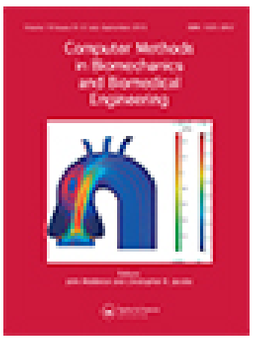

Taylor & Francis
Taylor & Francis Group

Computer Methods in Biomechanics and Biomedical Engineering

ISSN: 1025-5842 (Print) 1476-8259 (Online) Journal homepage: https://www.tandfonline.com/loi/gcmb20

Texture analysis of the 3D collagen network and automatic classification of the physiology of articular cartilage

Xiaojuan Duan, Jianping Wu, Benjamin Swift & Thomas Brett Kirk

To cite this article: Xiaojuan Duan, Jianping Wu, Benjamin Swift & Thomas Brett Kirk (2015) Texture analysis of the 3D collagen network and automatic classification of the physiology of articular cartilage, Computer Methods in Biomechanics and Biomedical Engineering, 18:9, 931-943, DOI: 10.1080/10255842.2013.864284

To link to this article: https://doi.org/10.1080/10255842.2013.864284

Computer Methods in Biomechanics and Biomedical Engineering, 2015
Vol. 18, No. 9, 931–943, http://dx.doi.org/10.1080/10255842.2013.864284

Taylor & Francis
Taylor & Francis Group

Texture analysis of the 3D collagen network and automatic classification of the physiology of articular cartilage

Xiaojuan Duan[a]*, Jianping Wu[b], Benjamin Swift[c] and Thomas Brett Kirk[b]

[a]*School of Mechanical and Chemical Engineering, The University of Western Australia, 35 Stirling Highway, Crawley, WA 6009 Perth, Australia;* [b]*Department of Mechanical Engineering, Curtin University, Kent Street, Bentley, WA 6102, Australia;* [c]*Research School of Computer Science, Australian National University, Canberra, Australia*

(*Received 24 August 2012; accepted 6 November 2013*)

A close relationship has been found between the 3D collagen structure and physiological condition of articular cartilage (AC). Studying the 3D collagen network in AC offers a way to determine the condition of the cartilage. However, traditional qualitative studies are time consuming and subjective. This study aims to develop a computer vision-based classifier to automatically determine the condition of AC tissue based on the structural characteristics of the collagen network. Texture analysis was applied to quantitatively characterise the 3D collagen structure in *normal* (International Cartilage Repair Society, ICRS, grade 0), *aged* (ICRS grade 1) and *osteoarthritic* cartilages (ICRS grade 2). Principle component techniques and linear discriminant analysis were then used to classify the microstructural characteristics of the 3D collagen meshwork and the condition of the AC. The 3D collagen meshwork in the three physiological condition groups displayed distinctive characteristics. Texture analysis indicated a significant difference in the mean texture parameters of the 3D collagen network between groups. The principle component and linear discriminant analysis of the texture data allowed for the development of a classifier for identifying the physiological status of the AC with an expected prediction error of 4.23%. An automatic image analysis classifier has been developed to predict the physiological condition of AC (from ICRS grade 0 to 2) based on texture data from the 3D collagen network in the tissue.

Keywords: texture analysis; automatic physical classification system; collagen structure; articular cartilage; osteoarthritis

1. Introduction

The mechanical properties of articular cartilage (AC) come from the integrity of its extracellular matrix, which is primarily composed of type II collagen and negatively charged proteoglycans. During joint articulation, AC experiences various compressive, shearing and wearing stresses. The collagen fibres are oriented differently between the surface and the deep zones to accommodate the different functional requirements of AC. They anchor to the subchondral bone, and align perpendicularly to the surface of AC in the radial zone. Functionally, they mainly participate in distributing loads and resisting compression (Roughley 2006). The collagen fibres are arched in the transitional zone to progressively contribute to shear and wear resistance. In the superficial zone, the distribution and structure of collagen fibres have been reported to appear more complex in 3D observations than depicted by traditional 2D microscopic studies. Two sub-layers have been classified in this zone (Jeffery et al. 1991; Hunziker et al. 2002; Hughes et al. 2005; Wu 2006). The most superficial layer, which is also called the lamina splendens, is integrated with an interwoven fibre network parallel to the articular surface (Wu et al. 2004), while the subjacent layer primarily contains collagen fibres oriented obliquely to the articular surface (Wu 2006).

While having a specific mechanical role in each zone, collagen fibres form a 3D scaffold that restrains the swelling pressure generated by proteoglycans so that the AC is provided with its overall mechanical properties. The deformation behaviours of AC under pressures have been modelled mathematically based on biphasic and triphasic theory (Mak et al. 1987; Mow et al. 1989; Lai et al. 1991), which confirmed experimentally that the disruption of the 3D collagen network plays an important role in changing the mechanical properties of AC. Fissures observed in the articular surface is a typical sign of early osteoarthritis (OA), which is directly associated with degeneration of the collagen fibres and their network in the superficial zone (Van der Sluijs and Van 1992; Ostergaard 1999; Pritzker et al. 2006). Because of this, studying the microstructure of the collagen network offers a way to assess the physiological properties of AC.

Some of the microscope techniques normally used to acquire images of objects are described below: (a) traditional light microscopy is the principal method used to obtain clear images of an object, but its utilisation is limited by refraction especially for identifying collagen fibres from proteoglycans that share a similar reflective index (Gratton EaV 1995). (b) Polarised and Phase Light Microscopes can only provide a general outline of the area

*Corresponding author. Email: xjd228@gmail.com

of interest but cannot reveal detail because of their relatively poor resolution (Bhosale and Richardson 2008). (c) Differential interference contrast microscopy is particularly suitable for acquiring the contour profile of living specimens, unstained and thick specimens (Harvath 1997). (d) Scanning electron microscopy has been the primary tool used to study the collagen fibres of AC. Transmission electron microscopy (TEM) can even distinguish individual collagen fibril (the molecular polymers) in AC. However, both of these types of electron microscopy (EM) require an extreme imaging environment that dehydrates AC and can alter the arrangement of collagen fibrils (Buckwalter and Mankin 1997).

Confocal microscopy cannot achieve the extremely high resolution required to detect an individual collagen fibril, and it acquires sufficient resolution compared to traditional light microscopy to explore the orientation of fibre bundles. It permits studying the three-dimensional internal microstructure of biological tissues with minimal physical disruption. By using fibre optic laser scanning confocal microscopy (Semwogerere and Weeks 2005) and Picrosirius red staining (which is a specific dye for collagen I, II and III), the 3D collagen scaffold in AC has been found to have a unique structure, which changes with the physiological status of AC. Confocal microscopy along with Picrosirius red staining had proved to give the best images of the collagen scaffold structure in AC compared to other optical microscopy techniques (Young et al. 1998).

Normal AC contains distinctive interwoven fibre bundles within the most superficial layer (Yeh et al. 2005; Duan et al. 2009; Mansfield et al. 2009), and the collagen fibres immediately adjacent align predominately in an oblique way to the articular surface (Wu 2003, 2006). The degeneration of AC is a complicated sequence that involves the changing of water content, cell apoptosis and necrosis, endogenous of enzymes and cells, and disruption and resynthesis of the extracellular matrix (Hough and Sokoloff 1997). Early OA shows signs of removal of the interwoven fibre bundles and alteration of the obliquely orientated collagen fibres towards perpendicular alignment. With increasing OA severity, there is clear disruption of the 3D collagen network.

Various histological/histochemical techniques that can grade the OA degree have been developed such as the pioneering work done by Collins (1949) and Mankin et al. (1971). However, the early scoring systems were formally questioned due to their reproducibility and their accuracy in the assessment of mild and earlier phases of OA (Van der Sluijs et al. 1992; Ostergaard et al. 1997). More standard OA model systems therefore were established leading to a more reliable scoring system to visually make the histological comparisons. Osteoarthritis Research Society International (OARSI) established a cartilage histopathology grading/staging system by examining the morphology changes and the proteoglycan content using cationic stains such as Safranin O or Toluidine Blue (Pritzker et al. 2006). However, including proteoglycan content as one of the criteria for OA grading has been questioned for its unpredictable performance because the fixation protocols and staining methods that are employed are believed to change the proteoglycan content and even the cell morphology when alcohol and acetone-based fixation protocols are used (Eggert et al. 1981; Hunziker et al. 1992; Hyllested et al. 2002). The International Cartilage Repair Society (ICRS) visual histological scoring system therefore endeavoured to standardize the fixation and staining techniques and made recommendations to apply buffered formalin and hematoxylin & eosin staining, respectively (Pousty et al. 1975).

Previous studies of the relationship between the 3D collagen network and the physiological status of AC have used mainly visual inspection of the corresponding histopathologic analysis (Anamalay et al. 1995; Wu et al. 2008). There has been a lack of quantitative analysis of the 3D collagen structure and automatic classification methods for assessing the physiological status of the AC. The present study discussed in this paper presents a 3D image analysis technique for quantifying the characteristics of the 3D collagen network in AC with physiological scores from ICRS grade 0 to 2. Texture parameters such as angular second moment (ASM), contrast, inverse different moment (IDM), correlation, and entropy are used to construct a feature vector representing the 3D collagen network in AC. Principle component and linear discriminant analysis of the texture data gives rise to a classifier for predicting the physiological status of the AC with an estimated prediction error of 4.23%.

2. Materials and methods

2.1 Specimen preparation

Forty-three cylindrical cartilage specimens of Ø 3 mm × 4 mm were punched out from the central weight-bearing zone of 11 bovine femoral condyles 6 h after slaughter. Twenty-two cartilage samples without visual disruption, presented with unevenly textured surface, were taken from five femoral heads of human cadavers aged between 40 and 60. A further 28 cartilage specimens showing minor OA signs presenting as soft indentions on the surface or superficial fissures were obtained from 15 human arthritic femoral heads after joint replacement surgeries. All the specimens were obtained with subchondral bone attached to prevent the natural distortion caused by the release of tensile stresses from the cartilage matrix.

Solutions of 0.2% phosphomolybdic acid and 1 g/l picrosirius red were applied at 4°C for 24 and 72 h, respectively, to the AC specimens which therefore had

been fixed to prevent any tissue degeneration in the future. The specimens were washed thoroughly in a 9 g/l saline solution, pH 7.4, and placed in specifically designed sample dishes to maintain the hydrated states while being observed for the collagen network using a fibre optic laser scanning confocal microscope (FOCM, Optiscan Pty Ltd, Melbourne, Australia) equipped with a 60X/NA 1.4 Olympus PlanApo oil immersion lens. The imaging was carried out using a reflectance channel and an illumination mode of 488 nm (50%) and 514 nm (50%) at an optical image step size of 0.689 or 0.756 μm. The acquired image stacks had 0.195 μm lateral and 0.23 μm axial resolutions. The imaging field of view was 33 μm^2. Fifty confocal image stacks were acquired from each physiological group.

The confocal image stacks were reconstructed into 3D images using Image J, shown as Figures 1–4(c), for 3D visual inspections, and image projections in the *XY*, *YZ* and

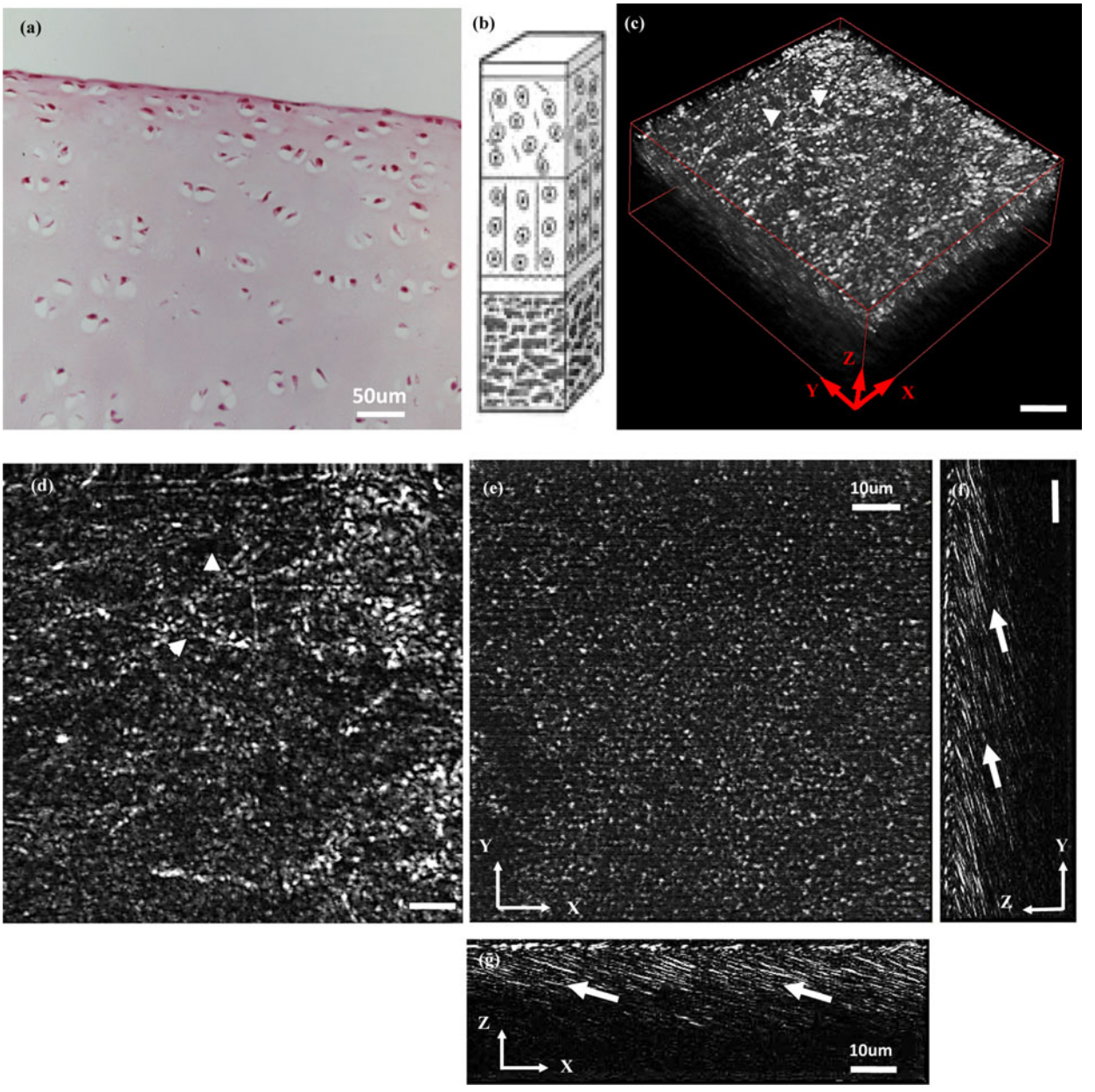

Figure 1. (a) H&E histology of ICRS grade 0 bovine AC. (b) Diagram of ICRS grade 0, normal cartilage. (c) The 3D collagen network in normal AC reconstructed from a confocal image stack. (d) The *XY* plane view of the 3D collagen network. (e) The *XY* plane view of the 3D collagen network after optically removing the interwoven fibre bundles in the lamina splendens. (f) The *YZ* plane view of the 3D collagen network. (g) The *XZ* plane view of the 3D collagen network. The arrows in f and g indicate the predominant orientation of the collagen fibres. White scale bar is 10 μm.

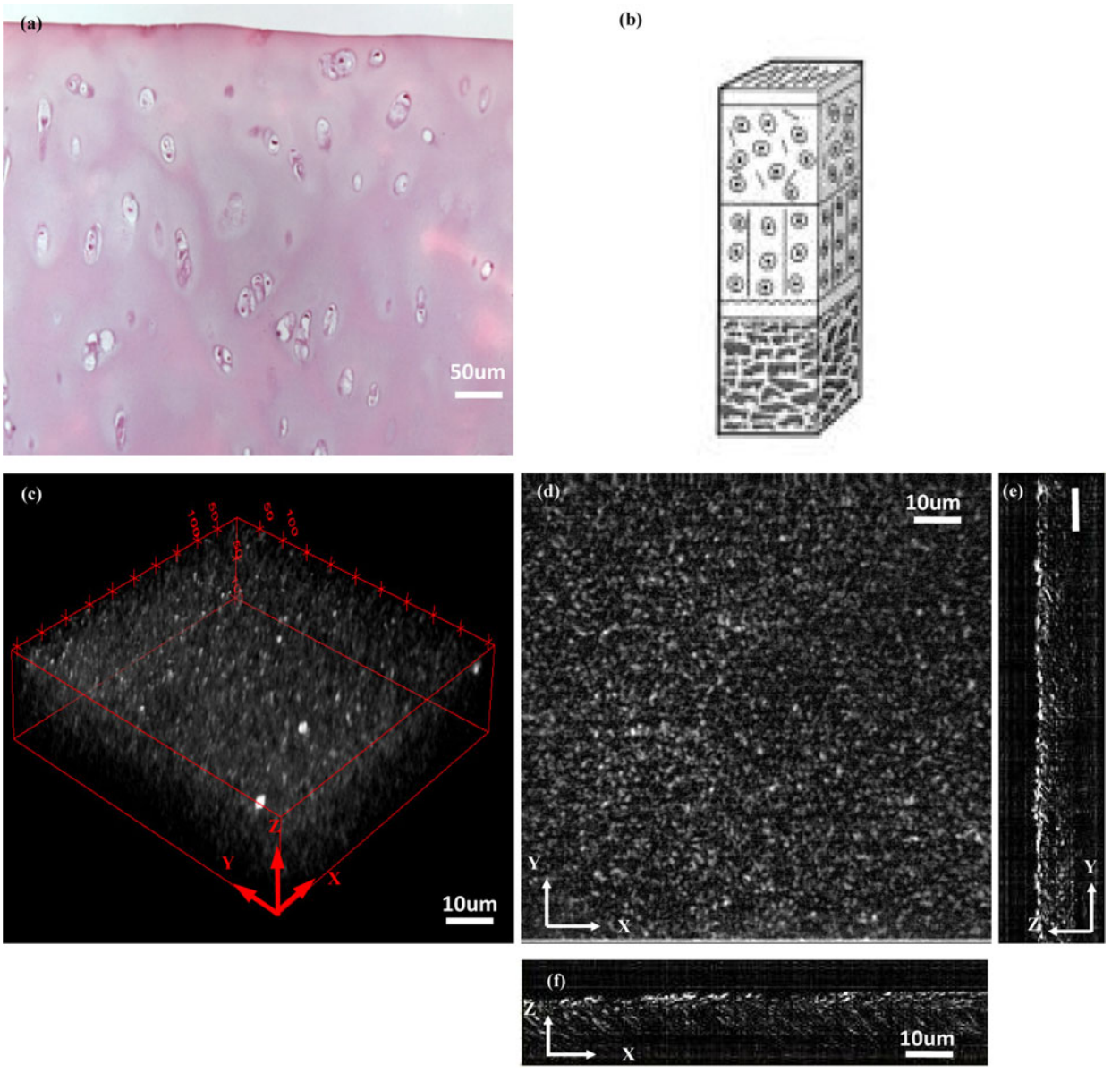

Figure 2. (a) H&E histology of ICRS grade 1 human AC. (b) Diagram of ICRS grade 1, nearly normal AC. (c) The 3D collagen networks in AC corresponding to ICRS grade 1. (d) The *XY* plane views of the 3D collagen networks. (e) The *YZ* plane views of the 3D collagen networks. (e) The *YZ* plane views of the 3D collagen networks. (f) The *XZ* plane views of the 3D collagen networks. White scale bars are 10 μm.

XZ plane, shown as Figures 1(e)–(g), 2(d)–(f), 3(d)–(f) and 4(d)–(f), for conducting a texture analysis three dimensionally on the collagen structures. Prior to the image analysis, the interwoven fibre bundles in the most superficial layer of normal AC, shown in Figure 1(c) and (d), were optically removed using F900e computer program (Optiscan Pty Ltd, Melbourne, Australia), shown in Figure 1(e). The interwoven fibre bundles have been studied previously for numerically identifying normal AC (Duan et al. 2009).

2.2 *Histology and International Cartilage Research Society grading*

Following the confocal microscopic imaging, the specimens were processed for H&E histology analysis using a stereo optical microscope (Zeiss Axioplan 2) to grade the physiological status of the AC in the scoring system established by the ICRS (Mainil-Varlet et al. 2003). The cartilage specimens were classified as normal, ICRS grade 0 which presented as an integral frictionless structure, shown in Figure 5.1(b); nearly normal, ICRS grade 1,

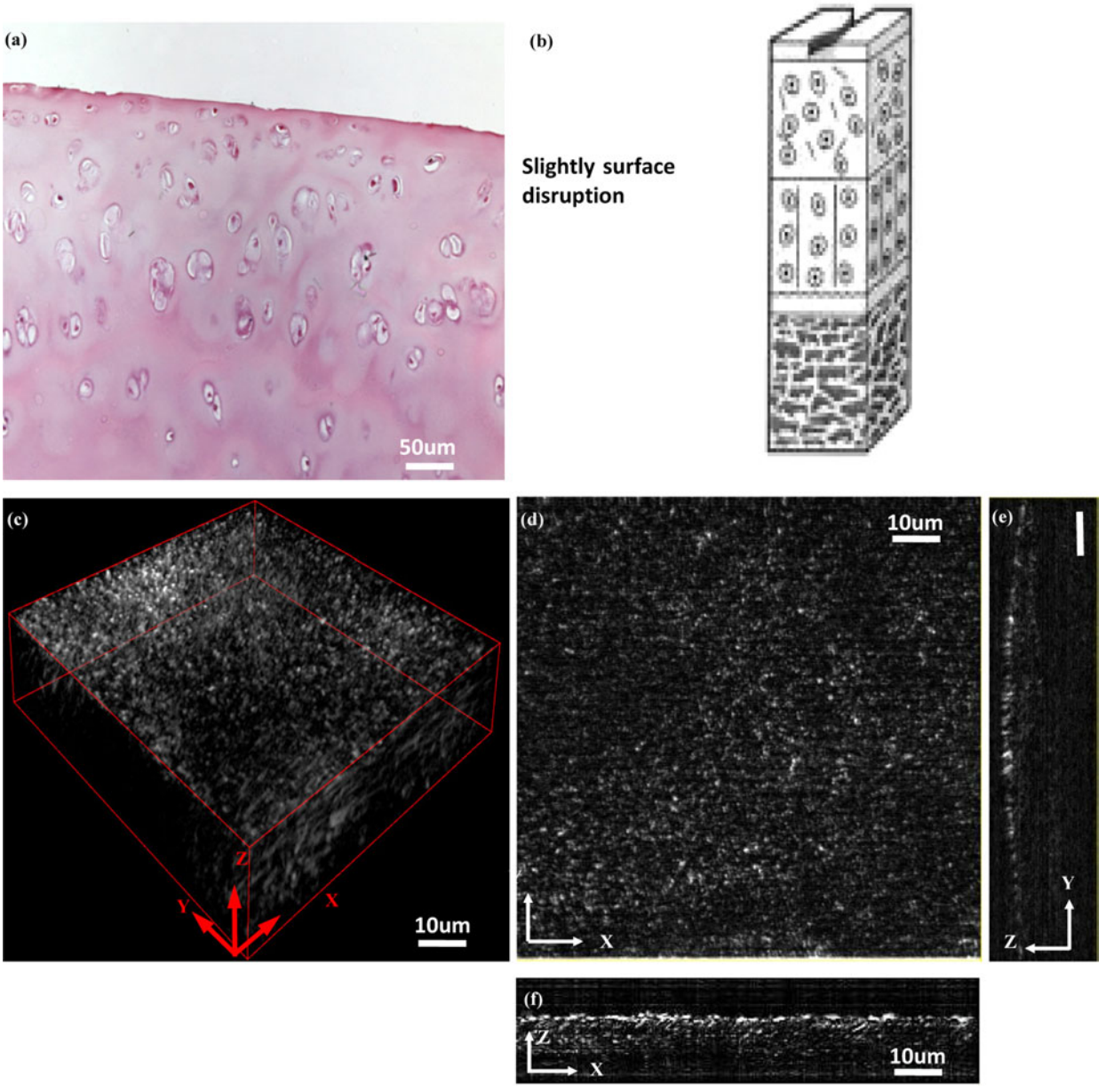

Figure 3. (a) H&E histology of ICRS grade 1 human AC. (b) Diagram of ICRS grade 1, nearly normal AC. (c) The 3D collagen networks in AC corresponding to ICRS grade 1. (d). The *XY* plane views of the 3D collagen networks. (e) The *YZ* plane views of the 3D collagen networks. (f) The *XZ* plane views of the 3D collagen networks. White scale bars are 10 μm.

shown in Figures 2(b) and 3(b) as soft indentation and/or superficial fissures on the cartilage surface; and abnormal, ICRS grade 2, shown as Figure 4(b) with a further surface lesion and the cracks which can extend down into upper part of the cartilage surface.

2.3 Texture analysis of the 3D collagen networks

The images reconstructed in the *XY*, *XZ* and *YZ* planes were conducted texture analysis of the 3D characteristics of the collagen network using Grey-level Co-occurrence Matrices (GLCM) (Haralick 1973). The GLCM achieved texture extractions by identifying the spatial variation within a local image region. Given an image I: $L_x \times L_y \rightarrow G$, where $L_x = \{1, 2, \ldots, N_x\}$ and $L_y = \{1, 2, \ldots N_y\}$ are the spatial domains in X and Y directions, while $G \in \{1, 2, \ldots, N_g\}$ is the grey levels domain. Then the GLCM P_d with a displacement vector of $\mathbf{d} = (d_x, d_y)$ is generated from image I as: $P_d(i,j) = |\{((r,s),(t,v)) : I(r,s) = i, I(t,v) = j\}|$, where $((r,s),(t,v)) \in L_x \times L_y$, and $(t,v) = (r + d_x, s + d_y)$, calculating the relative frequencies of a pair of pixels with a grey level of i and j with a

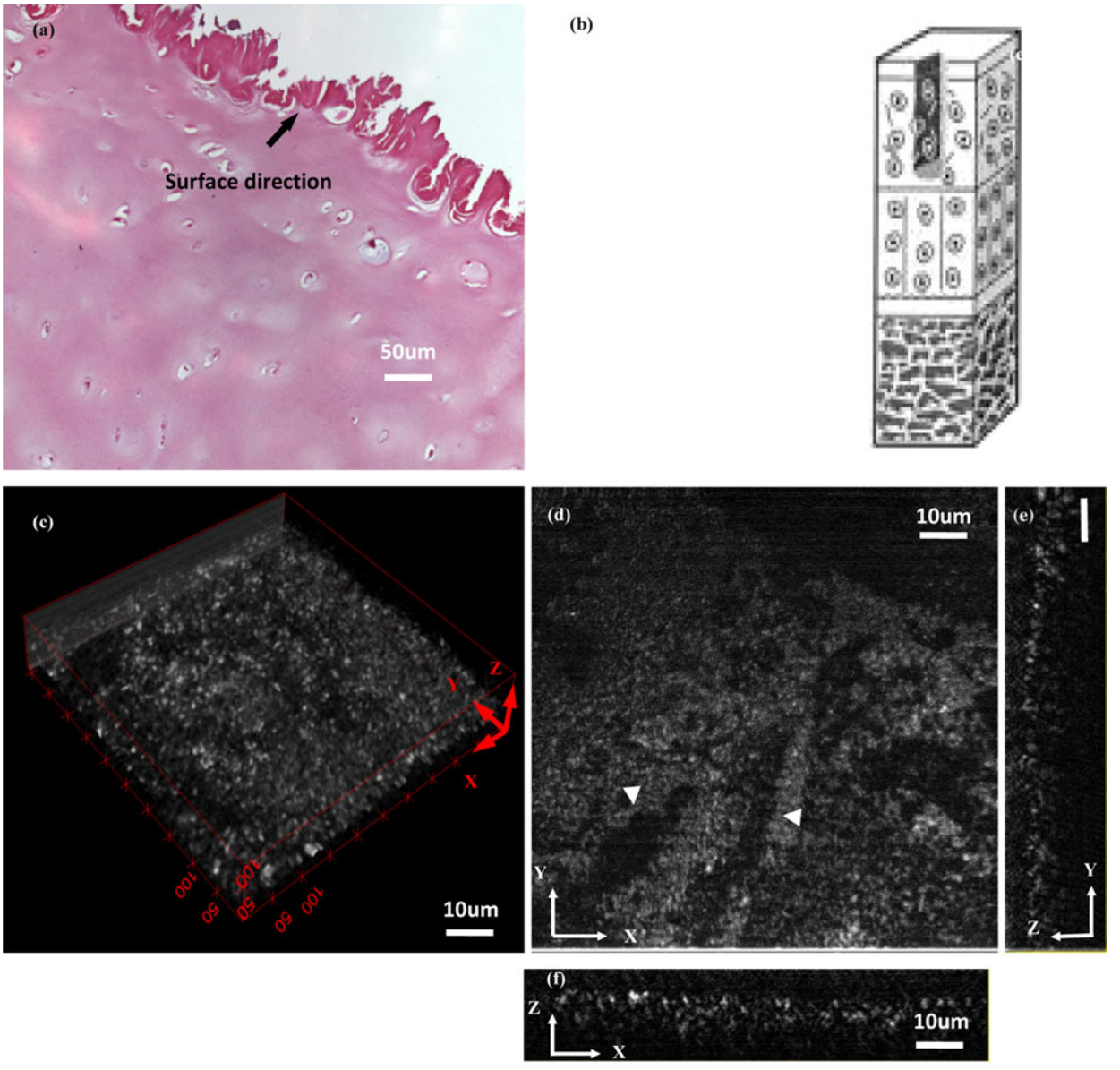

Figure 4. (a) H&E histology of the ICRS grade 2 human AC. (b) A diagram of ICRS grade 2. (c) The 3D image of the collagen network in ICRS grade 2 AC. (d) The *XY* plane view of the 3D collagen network. (e) The *YZ* plane view of the 3D collagen network. (f) The *XZ* plane view of the 3D collagen network. White scale bars are 10 μm.

distance of **d**. By changing the value of **d**, the co-occurrence matrix along different directions were acquired. For instance, when setting $\mathbf{d} = (1, 0)$, it produced a horizontal grey-level spatial dependence matrix at 0°. When $\mathbf{d} = (1, 1)$, it presented a grey-level spatial dependence matrix at 45°. Subsequently, the 90° and 135° matrices were generated by setting $\mathbf{d} = (0, 1)$ and $\mathbf{d} = (-1, 1)$ respectively.

For each of the specimens, five GLCM at 0° to 180° were generated at 45° intervals from the images in the *XY*, *XZ* and *YZ* plane, respectively, to analyse the texture features of the 3D collagen meshwork. Five texture featuring parameters of ASM, contrast, IDM, correlation and entropy were extracted from each of the matrices.

(1) ASM was given as $f_{\text{egy}} = \sum_{i=1}^{N_g} \sum_{j=1}^{N_g} P_d^2(i,j)$, which reflects the energy intensity of an image and measures the homogeneity of the image. The more homogeneous an image is, the larger the ASM becomes.

(2) Contrast was defined as $f_{\text{ctr}} = \sum_{i=1}^{N_g} \sum_{j=1} N_g(i-j)^2 P_d(i,j)$, which measures the amount of local intensity variations presented in an image. It

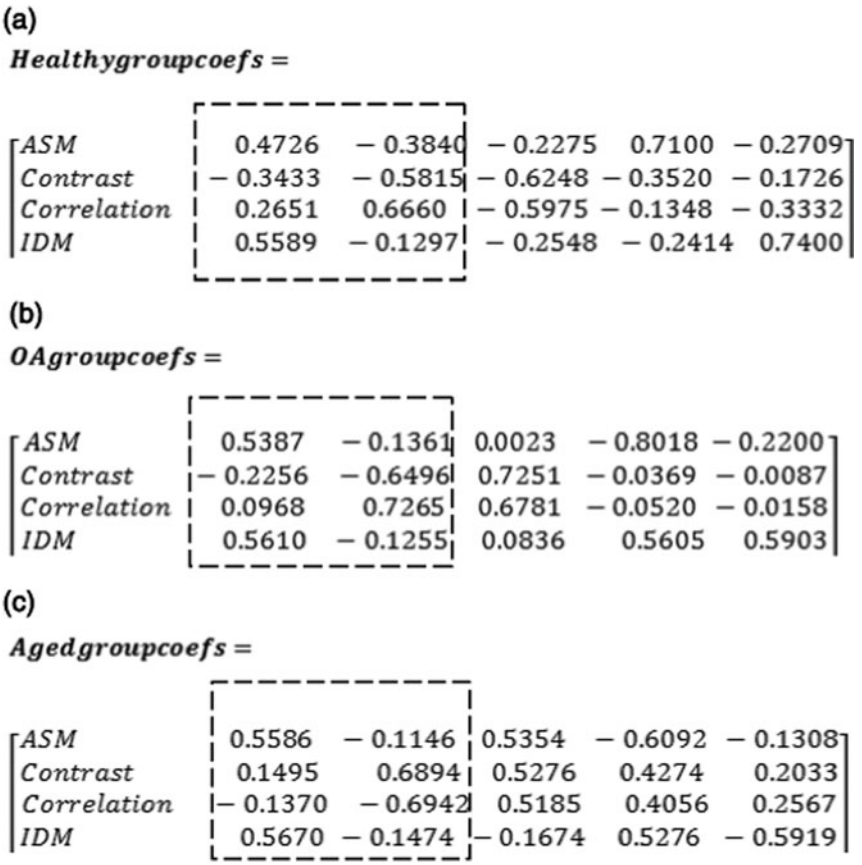

Figure 5. (a) The feature vectors of the normal cartilage group, corresponding to ICRS grade 0. (b) The feature vectors of the aged cartilage group, corresponding to ICRS grade 1. (c) The feature vectors of the OA cartilage group, corresponding to ICRS grade 2. The first two columns of the principle components highlighted by the dash squares possessed higher eigenvalues and were used for conducting the auto-classification of the physiological status of the specimens.

is often large when a pixel pair of (r,s) and(t,v) being compared has different intensity values.

(3) IDM: $f_{\text{hmg}} = \sum_{i=1}^{N_g}\sum_{j=1}^{N_g} P_d(i,j)/1+(i-j)^2$, which is large when a pair of pixels being compared have the same intensity value.

(4) Correlation: $f_{\text{cor}} = (\sum_{i=1}^{N_g}\sum_{j=1}^{N_g}(i-\mu_x)(j-\mu_y)P_d(i,j))/\sigma_x\sigma_y$, where μ_x and μ_y are the means and $\sigma_x\sigma_y$ are the standard deviations of $P_d(x)$and $P_d(y)$, respectively, with $P_d(x) = \sum_{j=1}^{N_g} P_d(x,j)$ and $P_d(y) = \sum_{i=1}^{N_g} P_d(i,y)$. Correlation measures the linear dependencies in the image.

(5) Entropy: $f_{\text{ent}} = -\sum_{i=1}^{N_g}\sum_{j=1}^{N_g} P_d(i,j)\log P_d(i,j)$, which measures the information content in an image. It will be large when the image contains more information.

2.4 Auto classification of the AC physiological status

The texture parameters acquired from the three physiological cartilage groups were then subjected to an auto-classification of the physiological status of the AC using linear discriminant analysis (LDA).

LDA is a statistical technique used to classify objects into mutually exclusive and exhaustive groups based on a set of measurable object features (Fisher 1936). The principle of this method is to reach the maximum 'between-classes' scatter S_b, Equation (1)

$$S_b = \sum_{i=1}^{c} n_i(u_i - u)(u_i - u)^T \tag{1}$$

and the minimum 'within-classes' scatter S_w, Equation (2)

$$S_w = \sum_{i=1}^{c}\sum_{x_k \in \text{class } i}(u_i - x_k)(u_i - x_k)^T, \tag{2}$$

where n_i is the number of the samples which belongs to class i, c is the number of classes, u_i is the mean of class i, u is the mean of the whole sample classes and x_k the kth sample. The procedure projected the sample class to a

lower vector space to maximize the separability. The projecting direction was generated by making Fisher's expression (3):

$$J_{\text{fisher}}(\varphi) = \frac{\varphi^{\mathrm{T}} S_{\mathrm{b}} \varphi}{\varphi^{\mathrm{T}} S_{\mathrm{w}} \varphi} \tag{3}$$

to reach its maximum vector φ (Fisher 1936). φ is an arbitrary vector in the reduced space.

While applying LDA to classify of the physiological characteristics of the AC specimens in this study, it was found to be difficult to form an optimal texture parameter combination that could systematically classify the three physiologically different cartilage groups completely from one processing. For instance, as shown in Figure 6(a) and (b), by randomly selecting two texture parameters, either the entropy and IDM or contrast and IDM, to carry out a LDA for an auto-classification of the three groups of cartilages, there was some overlap between the ICRS grade 1 cartilage from ICRS grade 2, while the ICRS grade 0 cartilage was almost completely separated from the ICRS 1 and ICRS 2 cartilages.

Both LDA and principle component analysis (PCA) were implemented in this study to classify the physiological status of the cartilage groups using the texture parameters. The PCA is appropriate in situations where the variables (e.g. the feature parameters) obtained for measurement contain some redundancy. This is the case when some of the variables are correlated with one another and need to be ranked according to their influence in the measurement so that an automatic classification can be efficiently carried out.

In this study, the redundancy in the feature vector may be attributable to the data collection method. The PCA

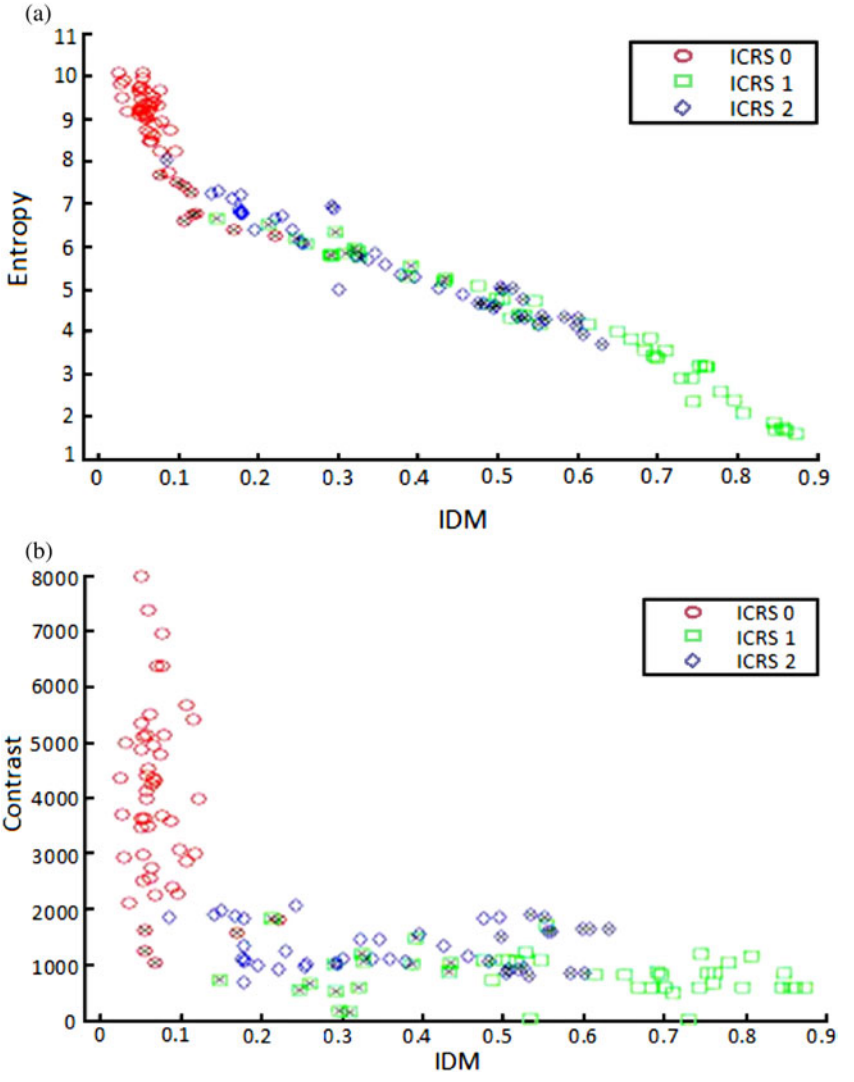

Figure 6. An automatic classifying system using either (a) LDA of entropy-IDM texture feature parameters or (b) LDA of contrast-IDM feature parameters did not separate the three cartilage groups completely. The system had a prediction error of 27.46%.

removes these correlations by finding the principle components of the covariance matrix of the texture parameters of all the samples (Pearson 1901). Through this procedure, the texture parameters obtained from the collagen texture analysis can be replaced by a smaller number of artificial variables, the principal components, which account for the majority of the variance in the observed variable (the texture parameters in this study). The principle components are then used as the predictors or criterion variables for distinguishing between the three cartilage groups with different physiological status using the LDA.

The covariance matrix is a matrix which contains the variance relationship between each variable (e.g. each feature parameter) in the measurement. Given an n dimensional column vector $\mathbf{X} = [X_1, X_2, \ldots, X_n]^{\mathrm{T}}$, the elements of the covariance matrix can be calculated using Equation (4):

$$\sum_{ij} = \mathrm{cov}(X_i, X_j) = \mathbf{E}\left[\left(X_i - \mu_i\right)\left(X_j - \mu_j\right)\right], \quad (4)$$

where μ_i is the mathematical expectation of X_i, i.e. $\mu_i = E(X_i)$. Therefore, the covariance matrix can be presented as Equation (5):

$$\mathbf{C} = \mathbf{E}[(\mathbf{X} - \mathbf{E}[\mathbf{X}])(\mathbf{X} - \mathbf{E}[\mathbf{X}])^{\mathrm{T}}]. \quad (5)$$

Eigenvalues λ and eigenvectors v will be generated by finding the non-zero vector which satisfies the equation: $\mathbf{C}v = \lambda v$ (Korn and Theresa 2000).

As the number of eigenvectors is same as the dimension of the matrix, the principle component of the data-set (the parameters) is the eigenvector with the highest eigenvalue. Then, a feature vector is the vector set where the eigenvectors are ranked by eigenvalues from the highest to lowest: $\mathrm{FeatureVector} = (\mathrm{eig}_1 \mathrm{eig}_2 \cdots \mathrm{eig}_n)$. Reductions of the correlations between the variables are achieved by abandoning some vectors with lower eigenvalues.

Five texture parameters obtained from a physiological group generated a 5×5 covariance matrix with five eigenvectors. Subsequently, the feature vectors of the three different physiological AC groups were obtained, as shown in Figure 5(a)–(c).

The privilege tendency of the parameters was reflected by the principle components. The first two columns of the principle components, the PC1 and PC2 highlighted by the dash squares in Figure 5, possessed higher eigenvalues. They were chosen for executing the LDA analysis. From here, the five feature parameters obtained from the texture analysis of the collagen networks in the three different physiological cartilage groups were able to be replaced by just two artificial parameters (X1 and X2) to carry out an auto-classification of the physiological status of the cartilage specimens without losing the most important information, as shown by Equation (6):

$$\begin{cases} X_1 = a_1x_1 + a_2x_2 + a_3x_3 + a_4x_4 + a_5x_5, \\ X_2 = b_1x_1 + b_2x_2 + b_3x_3 + b_4x_4 + b_5x_5, \end{cases} \quad (6)$$

where x_i ($i = 1, 2, 3, 4$ and 5) is the ith feature parameter. a_j and b_j ($j = 1, 2, 3, 4$ and 5) were composed of the first two principle components, which in short are presented by Equation (7):

$$\text{Component coefficients} = \begin{bmatrix} a_1 & a_2 & a_3 & a_4 & a_5 \\ b_1 & b_2 & b_3 & b_4 & b_5 \end{bmatrix}^{\mathrm{T}}. \quad (7)$$

As each of the parameters was given a weight after the PCA, shown as Equation (3), the two artificial feature parameters (X_1 and X_2) were generated by the matrix multiplication with the original parameter data-sets, shown as Equation (4). The two artificial vectors (PC1 and PC2) were then used to classify the physiological condition of the AC specimens using LDA, as shown in Figure 7.

The purpose of this study was to investigate the 3D collagen texture differentiation related to AC tissue degeneration, in order to provide a computer-aided classification system based on the variables that can be measured. Therefore, the ability of the developed classification system to detect the deterioration of AC through texture analysis needed to work well on different sample sources, and the results showed this was the case. As the texture analysis result varies from sample to sample of the same OA grade due to the biodiversity, to obtain an objective and statistically significant result, enough samples needed to be collected. Due to the limited ability of obtaining healthy human cartilage tissue, healthy bovine cartilages were sampled instead. The 150 collagen image stacks obtained from the three physiological groups (50 image stacks/group) were subjected to texture analysis using GLCM. The texture parameters obtained from 90 images (30 images/group) were used to train the classifier, and the remaining 60 images (20 images/group) were left out for validating the classifier.

3. Results

As shown by the 3D images in Figures 1–4, the 3D collagen networks from the different AC condition groups showed different structural characteristics. The 3D collagen network in normal AC showed high structural integrity, as indicated by interwoven fibre bundles (arrow heads) and neatly compact underlying collagen fibres, which aligned predominantly to be oblique to the surface of the AC, as shown in Figure 1. During progression of the physiological status from ICRS 0 to 1, the 3D collagen network gradually lost its structural integrity, as shown in

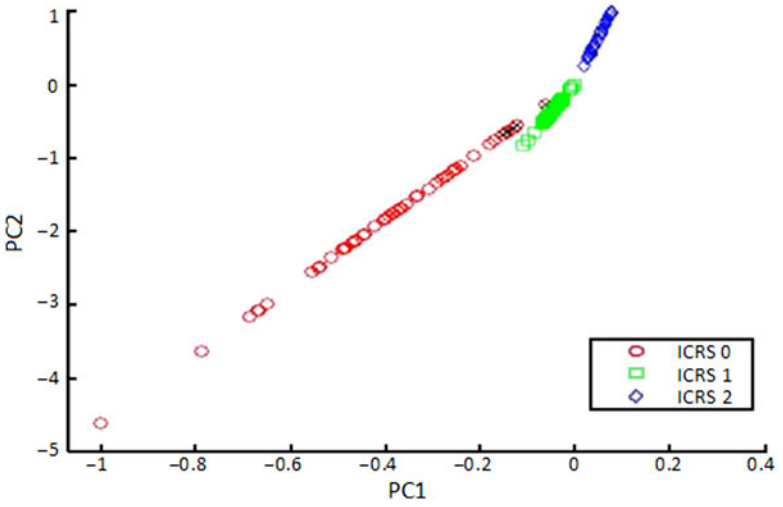

Figure 7. An automatic classification system based on using the two principle components and LDA permitted automatic classifying the AC with physiological status assessed as ICRS grade 0, ICRS grade 1 and ICRS grade 2. The system has a prediction error of 4.23%.

Figures 2(c) and 3(c). The interwoven fibre bundles gradually became less apparent in the 3D collagen. Also, the collagen fibres showed less directional orientation. When the physiological condition degraded to ICRS grade 2, an increase of the disruption of the 3D collagen framework became obvious, as seen in Figure 4(c). However, the apparent collagen structural alteration observed in the 3D images during an early physiological change of the AC from ICRS grade 0 to 1 could not be seen clearly in the 2D images in the *XY* location, see Figures 1(e), 2(d) and 3(d).

This study carried out a comprehensive texture analysis of the 3D collagen network in the three different physiological cartilage groups by studying the 3D collagen texture in the *XY*, *XZ* and *YZ* plane. The texture characteristics presented by obliquely distributed collagen fibres meshed as a network in its 3D natural view has been quantitatively measured by the parameters applied in the processing. Therefore, any 3D microstructure alteration of collagen fibres associated with the cartilage deterioration has been able to be captured and measured by applying the texture parameters and by tracking its variation. Fifty collagen networks acquired respectively from the three cartilage groups stated as ICRS grade 0 to 2 were quantitatively analysed. The results were shown in Table 1. Normal AC had a significantly higher mean contrast and entropy value in the 0° analysis. In comparison, the mean IDM value of the normal cartilage was much lower than the other two physiological groups, although the contrast value was not considerably different between the ICRS grade 1 and 2 groups. In the orthogonal directions (the *YZ* and *XZ*), the texture analysis showed that the mean value of ASM and IDM were inversely proportional to the healthy level of the AC, while the decrease in the mean value of the entropy was associated with the declining of the physiology of the AC.

In addition, the contrast measurement conducted in the *XZ* and *YZ* plane showed two peak values at 45° and 135° in normal AC, which approximately correspond to the predominant orientation of the collagen fibres underlying to the interwoven fibre bundles, shown in Figure 1(g) and (f). The contrast measurement of aged and OA cartilage

Table 1. The mean feature parameters of the three physiological AC groups (mean ± STD).

		ASM ($\times 10^{-3}$)	Contrast ($\times 10^{-3}$)	Correlation ($\times 10^{-3}$)	IDM ($\times 10^{-3}$)	Entropy
YZ plane	ICRS 0	2.94 ± 1.23	4.12 ± 2.79	0.12 ± 0.46	0.76 ± 0.39	8.57 ± 4.46
	ICRS 1	17.07 ± 6.58	0.81 ± 0.35	0.65 ± 0.28	2.65 ± 1.25	6.35 ± 3.25
	ICRS 2	62.35 ± 28.6	0.54 ± 0.19	1.90 ± 0.75	4.26 ± 2.03	4.98 ± 2.67
XZ plane	ICRS 0	3.72 ± 1.87	2.89 ± 1.43	0.19 ± 0.54	0.98 ± 0.47	8.52 ± 3.94
	ICRS 1	27.34 ± 13.4	0.59 ± 0.20	0.77 ± 0.37	3.42 ± 1.33	5.87 ± 2.08
	ICRS 2	94.12 ± 36.2	0.43 ± 0.17	1.17 ± 0.61	4.97 ± 2.84	4.57 ± 2.49
XY plane	ICRS 0	0.619 ± 0.39	2.68 ± 0.96	0.23 ± 0.17	0.63 ± 0.29	9.61 ± 5.26
	ICRS 1	4.553 ± 2.67	0.10 ± 0.33	4.45 ± 2.02	2.39 ± 1.12	6.68 ± 3.73
	ICRS 2	5.073 ± 3.04	0.14 ± 0.57	3.84 ± 1.35	2.09 ± 1.03	6.82 ± 3.62

Note: ICRS 0, normal cartilage; ICRS 1, aged cartilage; ICRS 2, OA cartilage.

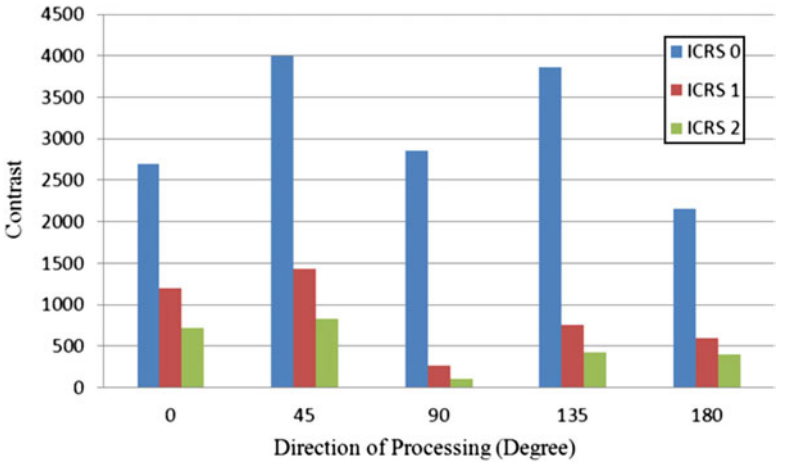

Figure 8. Contrast feature parameters of normal (ICRS 0), aged (ICRS 1) and OA (ICRS 2) cartilages. The contrast analysis of the normal cartilage showed two peaks at 45° and 135°, which indicated the predominant orientations of the collagen shown in Figure 1(f) and (g), respectively.

peaked evenly at 0°, 45°, 135° and 180°, shown in Figure 8 (b) and (c), respectively. This generally indicates that the collagen fibres are oriented evenly at these directions, as shown in Figures 3(e),(f) and 4(e),(f).

While the feature parameters obtained from the image analysis of the 3D collagen networks enabled quantifying the general physiological status of the three AC groups, it would be time consuming to analyse the substantial feature data during a time constrained medical diagnosis, as shown in Table 1. Therefore, an automatic classification system has been constructed to automatically assess the physiological status of cartilage specimens. The initial auto-classification methodology of using LDA and selecting two feature parameters at random did not produce good separation between the classes, as shown in Figure 6. Most ICRS grade 1 cartilage specimens were overlapped with the ICRS grade 2 cartilage specimens. The prediction error of this system was 27.46%, which is inadequate for use in a clinical setting.

The high unacceptable prediction error in diagnosis of 27.46% can be attributed to using only two texture parameters, and this was due to the high biodiversity of each individual sample reflected by large variance of each measured parameters, given as Table 1. For an auto-classification to be of use in a clinical setting, to quantify the condition of the collagen fibres in the 3D meshed network and to track their deterioration and hence onset of OA, it is important that there is a low margin of error, and that the results are repeatable. The purpose of the auto-classification system is to remove the subjectivity of interpretation and hence rely on the result produced by the classification system. Therefore, when all five parameters measured for each sample (ASM, contrast, IDM, correlation and entropy) were used in a PCA prior to the LDA procedure being applied, a much better separation between the groups can be achieved, as shown in Figure 7. Consequently, the margin of error in the auto classifier reduced significantly to 4.23% as more weighing factors have been taken into consideration.

In addition, the contrast measurement in the *XZ* and *YZ* direction approximated the collagen orientation characteristics of AC. As shown in Figure 8, the contrast parameter in normal AC showed two peak values at 45° and 135° in normal AC, which approximately corresponds to the predominant orientation of the collagen fibres underlying the interwoven fibre bundles in the normal AC, shown in Figure 1(f) and (g). However, there were no obvious peaks seen in the contrast graphs of aged and OA cartilage shown in Figure 8. This is consistent with the fact that the collagen fibres in the cartilage groups generally did not have preferred orientations, as shown in Figures 3 (e),(f) and 4(e),(f).

4. Discussion

Texture analysis has been widely used in many research fields, including material science, geography, aerial and satellite image analyses, to characterise the image patterns and identify useful information from the images. It has also played an important role in aiding medical diagnosis, such as pulmonary classification (Sutton and Hall 1972), the study of blood cells (Landeweerd and Gelsema 1978; Harms et al. 1986), identification of the abnormality shown by ultrasound imaging of the liver (Chen et al. 1989) and echocardiography (Chandrasekaran et al. 1989). For the first time, in this study, a texture analysis technique has been developed to quantitatively characterise the 3D collagen network in AC with physiological status scored as ICRS grade 0 to 2 as means of comprehensively quantifying the physiological status of early degraded

cartilage. This overcomes the subjective nature of the qualitative and semi-quantitative evaluation methods used in the medical field.

Since it is well accepted that the collagen fibres in AC are a 3D meshwork, it is crucial when examining the collagen structure to use 3D imaging and analysis techniques. As shown in Table 1, the mean texture feature parameters of the collagen network of the ICRS grade 1 and 2 cartilage group showed no significant diversity in the analysis carried out in the *XY* plane but they altered dramatically in the vertical direction analysis (the *YZ* and *XZ* planes). This clearly demonstrates the limitation of analysing the 3D collagen meshwork using only 2D techniques.

The distinct variation in the feature parameters of the three physiological cartilage groups has allowed development of a LDA classifier to automatically distinguish the physiological status of the cartilage in the three physiological states. As each feature parameter has a different influence in identifying the features of the 3D collagen networks in three physiological cartilage groups in 3D (the *XY*, *XZ* and *YX* direction), PCA was used to rank the power of the feature parameters in identifying the characteristics of the 3D collagen network. This also allows the feature parameters with a lower eigenvalue to be ignored. By using two highest eigenvalues identified by the PCA in the LDA, the classifier presented in this study has been shown to be useful for automatically identifying AC with early physiological changes shown at a microscopic level.

The current clinical diagnosis of OA is mainly based on the doctors' assessment of the pathological section of the patients' cartilage, which is subjective and time consuming. The system presented in this paper, however, has a potential application on integrating with confocal arthroscopy so that the physiological condition of AC can be obtained instantly by orthopaedic researchers without tissue biopsy (Jones et al. 2007). Although the prediction error of the classifier was reduced to 4.23% with the use of PCA, this prediction error is still high for usage of the system in medical diagnosis. By increasing the size of the training set and number of features, it may be possible in the future to reduce the system prediction error to an acceptable level for early OA diagnosis.

5. Conclusion

Confocal microscopy was used in this study because of its unique performance in living tissue imaging. Compared to conventional optical microscopy, which has insufficient imaging resolution to resolve the collagen fibres in AC, and EM, which has superior imaging resolution but damages the integrity of tissue structure, confocal microscopy can image the internal microstructure of AC with considerable resolution and minimal physical disturbance. The use of Picrosirius red provided a large increase in the birefringence properties of the collagen fibres in the AC (Smaill 1998).

This study developed an image analysis technique for confocal microscopy to quantify the texture characteristics of the 3D collagen matrices in three physiological states of AC scored as ICRS grade 0 to 2. The results revealed that 3D image analysis was capable of detecting differences in the collagen network in the cartilage groups. The use of PCA as a pre-processing step before the LDA resulted in a classifier that improves the ability to identify the physiological status of the AC, especially the subtle physiological change of AC during early OA.

Implementing such a classifier in an imaging system such as confocal arthroscopy, a fibre optic imaging technique employed by the laser confocal microscopy for real time histology in a clinical setting (Jones et al. 2004, 2007, 2008), would allow medical researchers to effectively diagnose the physiological status of AC and early OA. Furthermore, it may allow surgeons to quantify efficiently the pathology of AC in real time during surgery.

Acknowledgements

The authors would like to thank Prof. Kevin Murray from the School of Mathematics and Statistics at the University of Western Australia, for consulting the statistical analysis method, and the Centre for Microscopy, Characterisation and Analysis at the University of Western Australia for providing access to microscopy facilities.

References

Anamalay RV, Kirk TB, Panzera D. 1995. Numerical descriptors for the analysis of wear surfaces using laser scanning confocal microscopy. Wear. 181–183, Part 2:771–776.

Bhosale AM, Richardson JB. 2008. Articular cartilage: structure, injuries and review of management. Brit Med Bull. 87:77–95.

Buckwalter JA, Mankin HJ. 1997. Instructional course lectures, the american academy of orthopaedic surgeons – articular cartilage. Part I: tissue design and chondrocyte–matrix interactions. J Bone Joint Surg. 79(4):600–611.

Chandrasekaran K, Aylward PE, Fleagle SR, Burns TL, Seward JB, Tajik AJ, et al. 1989. Feasibility of identifying amyloid and hypertrophic cardiomyopathy with the use of computerized quantitative texture analysis of clinical echocardiographic data. J Am College Cardiol. 13:832–840.

Chen CC, DaPonte JS, Fox MD. 1989. Fractal feature analysis and classification in medical imaging. IEEE Trans Med Imaging. 8:133–142.

Collins DH. 1951. The pathology of articular and spinal diseases. J Bone Joint Surg. 33(3):819-a.

Duan XJ, Wu JP, Kirk TB. 2009. Identifying collagen bundles in the most superficial layer of normal articular cartilage. In: International conference on computational intelligence and software engineering. CiSE. p. 1–4.

Eggert FM, Linder JE, Jubb RW. 1981. Staining of demineralized cartilage. Histochemistry. 73:385–390.

Fisher RA. 1936. The use of multiple measurements in taxonomic problems. Ann Eug. 7:179–188.

Gratton EaV M. 1995. Laser source for confocal microscopy. In: Pawley J, editor. Handbook of biological confocal microscopy. New York (NY): Plenum Publishing Co..

Haralick RM. 1973. Textural features for image classification. IEEE Trans Syst Man Cybernet. 3:610–621.

Harms H, Gunzer U, Aus HM. 1986. Combined local color and texture analysis of stained cells. Comput Vis Graph Image Process. 33:364–376.

Harvath L. 1997. Overview of fluorescence analysis with the confocal microscope. In: Javois LC, editor. Methods in molecular biology. Totowa (NJ): Humana Press.

Hough AJ, Sokoloff L. 1997. Pathology of osteoarthritis. A textbook of rheumatology. Vol. 19 12th ed. Philadelphia (PA): Lea and Febiger. p. 3.

Hughes LC, Archer CW, Gwynn I. 2005. The ultrastructure of mouse articular cartilage: collagen orientation and implications for tissue functionality. A polarised light and scanning electron microscope study and review. Eur Cells Mater. 9:68–84.

Hunziker EB, Ludi A, Herrmann W. 1992. Preservation of cartilage matrix proteoglycans using cationic dyes chemically related to ruthenium hexaammine trichloride. J Histochem Cytochem. 40:909–917.

Hunziker EB, Quinn TM, Häuselmann HJ. 2002. Quantitative structural organization of normal adult human articular cartilage. Osteoarthr Cartilage. 10:564–572.

Hyllested JL, Veje K, Ostergaard K. 2002. Histochemical studies of the extracellular matrix of human articular cartilage—a review. Osteoarthr Cartilage. 10:333–343.

Jeffery A, Blunn G, Archer C, Bentley G. 1991. Three-dimensional collagen architechture in bovine articular cartilage. Brit Editorial Soc Bone Joint Surg. 73-B:795–801.

Jones CW, Keogh A, Smolinski D, Wu JP, Kirk TB, Zheng MH. 2004. Histological assessment of the chondral and connective tissues of the knee by a confocal arthroscope. J Musculoskelet Res. 8:75–86.

Jones CW, Smolinski D, Willers C, Yates PJ, Keogh A, Fick D, Kirk TB, Zheng MH. 2007. Laser scanning confocal arthroscopy of a fresh cadaveric knee joint. Osteoarthr Cartilage. 15:1388–1396.

Jones C, Willers C, Keogh A, Smolinski D, Fick D, Yates P, Kirk TB, Zheng MH. 2008. Matrix-induced autologous chondrocyte implantation in sheep: objective assessments including confocal arthroscopy. J Orthopaed Res. 26:292–303.

Korn GAK, Theresa M. 2000. Mathematical handbook for scientists and engineers: definitions, theorems, and formulas for reference and review. New York (NY): Dover Publications/ McGraw Hill. 1152 p.

Lai WM, Hou JS, Mow VC. 1991. A triphasic theory for the swelling and deformation behaviors of articular cartilage. J Biomech Eng. 113:245–258.

Landeweerd GH, Gelsema ES. 1978. The use of nuclear texture parameters in the automatic analysis of leukocytes. Pattern Recogn. 10:57–61.

Mainil-Varlet P, Aigner T, Brittberg M, Bullough P, Hollander A, Hunziker E, Kandel R, Nehrer S, Pritzker K, Roberts S, et al. 2003. Histological assessment of cartilage repair a report by the histology endpoint committee of the International Cartilage Repair Society (ICRS). J Bone Joint Surg. 85:45–57.

Mak AF, Lai WM, Mow VC. 1987. Biphasic indentation of articular cartilage—I. Theoretical analysis. J Biomech. 20:703–714.

Mankin H, Dorfman H, Lippiello L, Zarins A. 1971. Biochemical and metabolic abnormalities in articular cartilage from osteoarthritic human hips. II. Correlation of morphology with biochemical and metabolic data. J Bone Joint Surg Am. 53A:523–537.

Mansfield J, Yu J, Attenburrow D, Moger J, Tirlapur U, Urban J, Cui ZF, Winlove P. 2009. The elastin network: its relationship with collagen and cells in articular cartilage as visualized by multiphoton microscopy. J Anat. 215:682–691.

Mow VC, Gibbs MC, Lai WM, Zhu WB, Athanasiou KA. 1989. Biphasic indentation of articular cartilage—II. A numerical algorithm and an experimental study. J Biomech. 22:853–861.

Ostergaard K. 1999. Validity of histopathological grading of articular cartilage from osteoarthritic knee joints. Ann Rheum Dis. 58:208–213.

Ostergaard K, Petersen J, Andersen CB, Bendtzen K, Salter DM. 1997. Histologic/histochemical grading system for osteoarthritic articular cartilage. Reproducibility and validity. Arthritis Rheum. 40:1766–1771.

Pearson K. 1901. On lines and planes of closest fit to systems of points in space. Philos Mag. 2(6):559–572.

Pousty I, Bari-Khan M, Butler W. 1975. Leaching of glycosaminoglycans from tissues by the fixatives formalin-saline and formalin-cetrimide. Histochem J. 7:361–365.

Pritzker K, Gay S, Jimenez SA, Ostergaard K, Pelletier JP, Revell PA, Salter D, Berg WB. 2006. Osteoarthritis cartilage histopathology: grading and staging. Osteoarthr Cartilage. 14:13–29.

Roughley PJ. 2006. The structure and function of cartilage proteoglycans. PEJu Rroopuegahnl eCyells Mater. 12:92–101.

Semwogerere D, Weeks E. 2005. Confocal microscopy. Encyclopedia of Biomaterials and Biomedical Engineering. London: Academic Press. Vol. 426, p. 1–64.

Smaill YL. 1998. Extended confocal microscopy of myocardial laminae and collagen network. J Microsc. 192:139–150.

Sutton RN, Hall EL. 1972. Texture measures for automatic classification of pulmonary disease. IEEE Trans Comput. C-21:667–676.

Van der Sluijs JA, Van S. 1992. The reliability of the Mankin score for osteoarthritis. J Orthopaed Res. 10:58–61.

Van der Sluijs J, Geesink R, Van der Linden A, Bulstra S, Kuyer R, Drukker J. 1992. The reliability of the Mankin score for osteoarthritis. J Orthopaed Res. 10:58–61.

Wu J. 2003. Analysis of orientations of collagen fibers by novel fiber-tracking software. Microsc Microanal. 9(6):574.

Wu JP. 2006. Quantitative characterization of collagen orientation in the superficial zone for studying early degenerative changes in articular cartilage. J Musculoskelet Res. 10:1–12.

Wu JP, Kirk TB, Zheng MH. 2004. Assessment of three-dimensional architechture of collagen fibers in the superfical zone of bovine articular cartilage. J Musculoskelet Res (JMR). 8:167–179.

Wu JP, Kirk TB, Zheng MH. 2008. Study of the collagen structure in the superficial zone and physiological state of articular cartilage using a 3D confocal imaging technique. J Orthopaed Surg Res. 3:29–40.

Yeh AT, Hammer-Wilson MJ, Van Sickle DC, Benton HP, Zoumi A, Tromberg BJ, Peavy GM. 2005. Nonlinear optical microscopy of articular cartilage. Osteoarthr Cartilage. 13:345–352.

Young AA, Legrice IJ, Young MA, Smaill BH. 1998. Extended confocal microscopy of myocardial laminae and collagen network. J Microsc. 192:139–150.